Basic Research in Cardiology (2021) 116:58
https://doi.org/10.1007/s00395-021-00900-9

ORIGINAL CONTRIBUTION

Cardiomyocyte Na^+ and Ca^{2+} mishandling drives vicious cycle involving CaMKII, ROS, and ryanodine receptors

Bence Hegyi[1] · Risto-Pekka Pölönen[1,2] · Kim T. Hellgren[1] · Christopher Y. Ko[1] · Kenneth S. Ginsburg[1] · Julie Bossuyt[1] · Mark Mercola[2] · Donald M. Bers[1]

Received: 14 July 2021 / Revised: 8 September 2021 / Accepted: 30 September 2021 / Published online: 14 October 2021

Abstract

Cardiomyocyte Na^+ and Ca^{2+} mishandling, upregulated Ca^{2+}/calmodulin-dependent kinase II (CaMKII), and increased reactive oxygen species (ROS) are characteristics of various heart diseases, including heart failure (HF), long QT (LQT) syndrome, and catecholaminergic polymorphic ventricular tachycardia (CPVT). These changes may form a vicious cycle of positive feedback to promote cardiac dysfunction and arrhythmias. In HF rabbit cardiomyocytes investigated in this study, the inhibition of CaMKII, late Na^+ current (I_{NaL}), and leaky ryanodine receptors (RyRs) all attenuated the prolongation and increased short-term variability (STV) of action potential duration (APD), but in age-matched controls these inhibitors had no or minimal effects. In control cardiomyocytes, we enhanced RyR leak (by low [caffeine] plus isoproterenol mimicking CPVT) which markedly increased STV and delayed afterdepolarizations (DADs). These proarrhythmic changes were significantly attenuated by both CaMKII inhibition and mitochondrial ROS scavenging, with a slight synergy with I_{NaL} inhibition. Inducing LQT by elevating I_{NaL} (by Anemone toxin II, ATX-II) caused markedly prolonged APD, increased STV, and early afterdepolarizations (EADs). Those proarrhythmic ATX-II effects were largely attenuated by mitochondrial ROS scavenging, and partially reduced by inhibition of CaMKII and pathological leaky RyRs using dantrolene. In human induced pluripotent stem cell-derived cardiomyocytes (hiPSC-CMs) bearing LQT3 mutation SCN5A N406K, dantrolene significantly attenuated cell arrhythmias and APD prolongation. Targeting critical components of the Na^+–Ca^{2+}–CaMKII–ROS–I_{NaL} arrhythmogenic vicious cycle may exhibit important *on*-target and also *trans*-target effects (e.g., I_{NaL} and RyR inhibition can alter I_{NaL}-mediated LQT3 effects). Incorporating this vicious cycle into therapeutic strategies provides novel integrated insight for treating cardiac arrhythmias and diseases.

Keywords Heart failure · Electrophysiology · Calcium · CaMKII · RyR · ROS

Abbreviations

AIP	Autocamtide-2-related inhibitory peptide
AP	Action potential
APD	Action potential duration
APD_{90}	Action potential duration at 90% repolarization
ATX-II	Anemone toxin II
CaMKII	Ca^{2+}/calmodulin-dependent kinase II
CaT	Ca^{2+} transient
CPVT	Catecholaminergic polymorphic ventricular tachycardia
DAD	Delayed afterdepolarization
EAD	Early afterdepolarization
hiPSC-CM	Human induced pluripotent stem cell-derived cardiomyocyte
HF	Heart failure
I_{K1}	Inward rectifier K^+ current
I_{Ks}	Slow delayed rectifier K^+ current
I_{NaL}	Late Na^+ current
ISO	Isoproterenol
LQT	Long QT
mitoROS	Mitochondrial reactive oxygen species
NCX	Na^+/Ca^{2+} exchanger
ROS	Reactive oxygen species
RyR	Ryanodine receptor
sAP	Spontaneous action potential

✉ Donald M. Bers
dmbers@ucdavis.edu

[1] Department of Pharmacology, University of California, Davis, 451 Health Sciences Drive, Davis, CA 95616, USA

[2] Cardiovascular Institute and Department of Medicine, Stanford University, Stanford, CA 94305, USA

sCaR	Spontaneous SR Ca^{2+} release
SR	Sarcoplasmic reticulum
STV	Short-term variability
WT	Wild-type

Introduction

Heart failure (HF) is characterized by cardiomyocyte Na^+ and Ca^{2+} dysregulation including elevated intracellular $[Na^+]$ ($[Na^+]_i$) and late Na^+ current (I_{NaL}), reduced sarcoplasmic reticulum (SR) Ca^{2+} uptake, and increased diastolic SR Ca^{2+} leak, Na^+/Ca^{2+} exchange (NCX), and reactive oxygen species (ROS) that contribute to systolic dysfunction and arrhythmias [1, 2, 8, 27, 54]. These alterations also frequently occur in many other heart diseases such as atrial fibrillation [47], ischemia/reperfusion injury [56], hypertrophic cardiomyopathy [6], long QT (LQT) syndromes [48], catecholaminergic polymorphic ventricular tachycardia (CPVT) [32, 70], and diabetes [16, 25]. Moreover, Ca^{2+}/calmodulin-dependent protein kinase δ (CaMKIIδ) is also upregulated and chronically active in these diseases [1, 20, 61], and directly promotes I_{NaL} [67] and diastolic SR Ca^{2+} leak through the ryanodine receptor (RyR) [1]. Furthermore, reactive oxygen species (ROS) are increased by CaMKII [49], and elevated $[Na^+]_i$ and intracellular $[Ca^{2+}]$ ($[Ca^{2+}]_i$) [7], which in turn further stimulate CaMKII [11] and RyR leak [50]. Thus, these pathological changes in HF are connected via a vicious cycle of positive feedback reinforcing systolic and diastolic dysfunction and arrhythmia mechanisms [18, 45, 68] (see Fig. 1). For example, a primary increase in SR Ca^{2+} leak would promote CaMKII activation, which can promote I_{NaL}, prolong action potential duration (APD), increase $[Na^+]_i$, and ROS production that can further drive the cycle and amplify the functional impacts of initial insults at any given point.

Based on the highly integrative nature of the vicious cycle and the significant impact it has on pathophysiological development, we hypothesized that targeting one of the key components (or combination of those) can prevent cellular proarrhythmia. Inhibition of one component in the vicious cycle with a selective drug is expected to induce the drug-specific *on*-target effect but also *trans*-target effects in the loop as it may reduce the feedback activation of the vicious cycle. The *on*-target drug effects have been the focus of research in recent decades and showed benefits in HF. (1) Selective Na^+ channel inhibitors (tetrodotoxin, GS-967) were shown to reverse the increased I_{NaL} and the prolongation of the APD in HF [27, 43]. (2) CaMKII inhibition using KN-93 or autocamide-2-related inhibitory peptide (AIP) was shown to reduce RyR leak (for matched SR Ca^{2+} load) in rabbit HF [1], and reduced diastolic Ca^{2+} spark rate in human HF [59]. (3) Mitochondrial-targeted antioxidant MitoTEMPOL normalized global cellular ROS and prevented arrhythmogenic remodelling in a guinea pig model of nonischaemic HF [9]. (4) The pathological leaky conformation of RyR, induced by CaMKII and ROS, can be selectively inhibited using dantrolene, which reduces SR Ca^{2+} leak in CPVT and HF [64]. However, the *trans*-target effects and the strengths of interactions in this vicious cycle have not been systematically investigated.

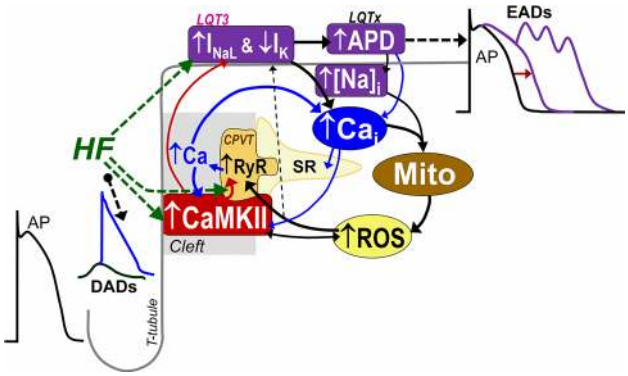

Fig. 1 Schematic of arrhythmogenic vicious cycle in heart disease. Heart failure (HF) is characterized by increases of ryanodine receptor (RyR) mediated Ca^{2+} leak, Ca^{2+}/calmodulin-dependent kinase II (CaMKII) activity, late Na current (I_{NaL}), intracellular $[Na]_i$, action potential duration (APD) and reactive oxygen species (ROS) production, along with reduced repolarization reserve (K^+ currents, I_K). These factors form a vicious positive feedback cycle that perpetuates HF-associated dysfunction and arrhythmogenesis. For example, the RyR Ca^{2+} leak increases local $[Ca^{2+}]$, further activating cleft CaMKII that further enhances RyR leak and I_{NaL} (red arrows) and downregulates K^+ channel expression to reduce I_K, which prolongs APD (as in genetic long QT (LQT) syndromes). Long APDs predispose myocytes to early afterdepolarizations (EADs) and increased intracellular $[Na^+]$ and $[Ca^{2+}]$ loading, which impairs mitochondrial Ca^{2+} handling and may further promote ROS production. ROS can further promote I_{NaL} and pathological leaky RyR (as in catecholaminergic polymorphic ventricular tachycardia, CPVT), and increase propensity for delayed afterdepolarizations (DADs). ROS also induces autonomous CaMKII activation closing the positive feedback loop

Here we measured the contribution of the $[Na^+]_i$–$[Ca^{2+}]_i$–ROS–CaMKII–RyR leak feedback interactions to proarrhythmic electrophysiological changes in HF rabbits [22]. We also assessed drug-induced RyR leak (mimicking CPVT, [18]) and enhanced I_{NaL} (mimicking long QT3, [24]) in control rabbit cardiomyocytes, and in human induced pluripotent stem cell-derived cardiomyocytes (hiPSC-CMs) carrying arrhythmogenic SCN5A N406K mutation [60].

Methods

Rabbit cardiomyocyte isolation

Enzymatic isolation of left ventricular cardiomyocytes from New Zealand White rabbits (male, 3–4-month-old)

was performed as previously described [21]. Briefly, animals were injected with heparin (400 U/kg body weight) and anesthetized with isoflurane (3–5%). Hearts were excised and retrograde perfused on constant flow Langendorff apparatus (5 min, 37 °C) with Ca^{2+}-free normal Tyrode's solution, gassed with 100% O_2. Then, ventricular myocytes were digested using collagenase type II (Worthington) and protease type XIV (Sigma-Aldrich). Ventricular myocytes were dispersed mechanically and filtered through a nylon mesh and allowed to sediment for ~ 10 min. The sedimentation was repeated three times using increasing [Ca^{2+}] from 0.125 to 0.25 then 0.5 mmol/L. Finally, ventricular myocytes were kept in Tyrode's solution at room temperature until use.

HF rabbit model

HF was induced in New Zealand White rabbits (male, 3–4-month-old) by aortic insufficiency and 4 weeks later by aortic constriction as previously described [22]. Data here reported were obtained from 10 HF and 10 age-matched control rabbits at 2–2.5 years of age. Echocardiography was performed periodically to monitor cardiac function. Cardiomyocytes were isolated from HF rabbits when left ventricular end-systolic dimension exceeded 1.45 cm. HF animals exhibited significant myocardial hypertrophy, enlarged left ventricular dimensions, pulmonary congestion, and abdominal ascites fluid accumulation, similar to our previous studies on this HF rabbit model [22, 54].

Human iPSC-CMs

Patient specific hiPSC line carrying the SCN5A N406K mutation was generated as previously described [60]. Human iPSC-CMs were differentiated by methods developed in the laboratory of Mark Mercola [44]. At day 20, hiPSC-CMs were placed in a metabolic maturation media and cultured for 5 weeks to improve cardiomyocyte phenotype, including more negative diastolic membrane potentials and Na^+ current dependent action potentials [12]. Then, hiPSC-CM monolayers were dissociated and re-plated in low density onto Matrigel-coated coverslips 3–5 days before experiments.

Electrophysiology

Following cell isolation, single cardiomyocytes were transferred to a temperature-controlled chamber (Warner Instruments, Holliston, MA, USA) mounted on a Leica DMI3000 B inverted microscope (Leica Microsystems, Buffalo Grove, IL, USA) and continuously perfused (2 mL/min) with Tyrode's solution containing (in mmol/L): NaCl 140, KCl 4, $CaCl_2$ 1.8, $MgCl_2$ 1, HEPES 5, Na-HEPES 5, glucose 5.5; pH = 7.40. Electrodes were fabricated from borosilicate glass (World Precision Instruments, Sarasota, FL, USA) having tip resistances of 2–2.5 MΩ when filled with internal solution containing (in mmol/L): K-aspartate 100, KCl 30, NaCl 8, Mg-ATP 5, phosphocreatine-K_2 10, HEPES 10, EGTA 0.01, cAMP 0.002, and calmodulin 0.0001; pH = 7.20 (with KOH). Using this internal solution, the intracellular Ca^{2+} transient and contraction of the cardiomyocyte were preserved [23]. Axopatch 200B amplifier (Axon Instruments Inc., Union City, CA, USA) was used for recordings, and the signals were digitized at 50 kHz by a Digidata 1322A A/D converter (Axon Instruments) under software control (pClamp10.4). The series resistance was typically 3–5 MΩ, and it was compensated by 90%. Experiments were discarded when the series resistance was high or increased by > 10%. Reported voltages are corrected for liquid junction potential. All experiments were conducted at 37 ± 0.1 °C.

Action potentials (APs) were evoked by 2-ms-long suprathreshold depolarizing pulses delivered via the patch pipette. 50 consecutive APs were recorded to examine the average behaviour, and APD at 90% repolarization (APD_{90}) was determined. Series of 50 consecutive APs were analysed to estimate short-term variability of APD_{90} (STV) according to the following formula: $STV = \Sigma(\left| APD_{n+1} - APD_n \right|)/[(n_{beats}-1)\times\sqrt{2}]$, where APD_n and APD_{n+1} indicate the durations of the nth and $(n+1)$th APs, and n_{beats} denotes the total number of consecutive beats analysed. APD alternans magnitude was calculated as the difference between the average APD_{90} of odd and even numbered beats during 50 consecutive APs recorded. Diastolic arrhythmogenic activities were elicited by cessation of 1-min tachypacing, and membrane potential was recorded for additional 1 min. Delayed afterdepolarizations (DADs) were defined as > 1 mV depolarization within 0.5 s. Spontaneous APs (sAPs) were defined as depolarizations showing overshoot with a fast upstroke phase. Early afterdepolarizations (EADs) were assessed at 0.2 Hz pacing, and EADs were defined as > 3 mV depolarization during AP repolarization.

AP-clamp experiments were performed to measure I_{NaL} as previously described [19]. A typical rabbit AP was used to AP-clamp cells at 2 Hz pacing frequency. I_{NaL} was measured as GS-967 (1 µmol/L)-sensitive current in control and following enhancement with ATX-II (5 nmol/L).

Cell pretreatments with MitoTEMPOL and AIP (myristoylated) started 30 min before the experiments, and the drugs were also added to both the perfusion and pipette solutions.

Chemicals and reagents were purchased from Sigma-Aldrich (St. Louis, MO, USA), if not specified otherwise. ATX-II and MitoTEMPOL were from Abcam (Cambridge, MA, USA), and GS-967 was from Cayman Chemical (Ann Arbor, MI, USA).

Calcium imaging

To measure SR Ca^{2+} concentration ($[Ca^{2+}]_{SR}$), freshly isolated rabbit cardiomyocytes were loaded with 8 µmol/L Mag-Fluo-4-AM (Invitrogen, Carlsbad, CA, USA) with 0.2% Pluronic F-127 (Biotium, Hayward, CA, USA) for 2 h at room temperature. Subsequently, cells were washed twice in fresh Tyrode's solution for 30 min to allow de-esterification to occur. Then, cardiomyocytes were placed in a narrow bath chamber with embedded field stimulation electrodes (RC-27NE2, Warner Instruments) and stimulated at 0.5 Hz frequency in Tyrode's solution at room temperature (22 ± 1 °C). Mag-Fluo-4 was excited at 480 nm wavelength using an Optoscan monochromator (Cairn Research, Faversham, UK) and fluorescence emission was collected at 535 ± 15 nm.

To measure $[Ca^{2+}]_i$, cardiomyocytes were loaded with 10 µmol/L Rhod2-AM (ThermoFisher, Waltham, MA, USA) for 10 min at room temperature and subsequently left to de-esterify in fresh Tyrode's solution for a minimum of 30 min. Then, cardiomyocytes were placed in a RC-27NE2 recording chamber and stimulated at 0.5 Hz frequency in Tyrode's solution at room temperature. Rhod2 was excited at 561 nm wavelength using an Optoscan monochromator, and fluorescence was collected at 530 ± 20 nm. Fluorescence signals were recorded after steady state was reached in the cell during pacing.

Statistical analysis

Data are presented as Mean ± SEM. Statistical significance of differences for normally distributed data was tested by paired Student's *t*-test to compare two groups and ANOVA with Dunnett's or Tukey's post-hoc test to compare multiple groups. For non-normally distributed data, we used Wilcoxon matched-pairs signed rank test, Mann–Whitney test, and Kruskal–Wallis ANOVA with Dunn's post-hoc test. Differences were deemed significant if $P < 0.05$.

Results

Enhanced RyR leak, CaMKII, and I_{NaL} all contribute to arrhythmogenic AP changes in HF

Cardiomyocytes in our HF rabbit model exhibited significantly prolonged APD_{90} and greater short-term APD variability (STV) vs. age-matched healthy controls at 1 Hz at 37 °C (Fig. 2a–d). We tested the effects of specific inhibition of either CaMKII, I_{NaL} or RyR leak on APs of rabbit ventricular myocytes isolated from failing and healthy hearts. Pretreatment with the selective CaMKII inhibitor peptide AIP (1 µmol/L) or the late Na^+ current inhibitor GS-967 (1 µmol/L) significantly shortened APD_{90} and reduced STV in failing myocytes to the level of healthy age-matched myocytes (Fig. 2a–d). Interestingly, the pathological RyR conformation inhibitor dantrolene (10 µmol/L) also shortened APD_{90} and reduced STV in HF (Fig. 2a–d). Importantly, in healthy control myocytes neither AIP nor dantrolene had significant effects on APD_{90}, and GS-967 only slightly shortened APD_{90} in healthy myocytes (Fig. 2c). In healthy myocytes GS-967 and AIP slightly reduced STV, but those differences were quantitatively small compared to those for HF myocytes (Fig. 2d). The effects of direct I_{NaL} inhibition (GS-967) and CaMKII (AIP) on APD and STV could be expected because I_{NaL} and CaMKII activity are known to be elevated in HF, and CaMKII has been shown to directly enhance I_{NaL} [5, 27, 67]. However, the potent effect of dantrolene on APD and STV is evidence that the pathological RyR state in HF increases APD and STV, which may be mediated by the vicious cycle via SR Ca^{2+} leak-promoted CaMKII and I_{NaL}.

RyR leak increases APD-variability via mitoROS-CaMKII-I_{NaL} feedback

To separate RyR leak from the complex HF phenotype, in terms of the arrhythmogenic feedback signalling network (i.e., the vicious cycle), we induced RyR leak by low [caffeine] (200 µmol/L) and isoproterenol (ISO; 100 nmol/L) in healthy rabbit ventricular myocytes. Caffeine (3 min) slightly prolonged APD_{90} and increased STV (Fig. 3a, b). The additional application of GS-967 decreased APD_{90} and STV back to control suggesting a role for Ca^{2+}-dependent upregulation of I_{NaL} (Fig. 3a, b). In contrast to caffeine effects, ISO (3 min) shortened APD_{90} and reduced STV (Fig. 3c, d). Then, inhibition of the slow delayed rectifier K^+ current (I_{Ks}) using HMR-1556 (HMR, 1 µmol/L) in the presence of ISO markedly prolonged APD_{90} (mimicking LQT1) and significantly increased STV, while HMR had no effect on APD_{90} at basal conditions without ISO stimulation (Fig. 3c, d). These data suggest that the upregulation of I_{Ks} counterbalances the increased I_{NaL} during β-adrenergic stimulation. Nonetheless, during steady-state pacing at 1 Hz, only very few DADs occurred in a small fraction of cells treated with either caffeine or ISO alone (Fig. 3e, f). However, when caffeine and ISO were applied together, several DADs were observed in every cell measured (Fig. 3e, f). This suggests that the increased SR Ca^{2+} leak (caffeine) must be combined with enhanced SR Ca^{2+} loading (ISO) to induce DADs in healthy myocytes. Hence, in the following, we used a combination treatment of low [caffeine] and ISO to investigate the role of the vicious cycle in proarrhythmic AP changes.

Following 3-min caffeine + ISO treatment, the AP plateau was significantly elevated (Fig. 4a), but the APD_{90} did not

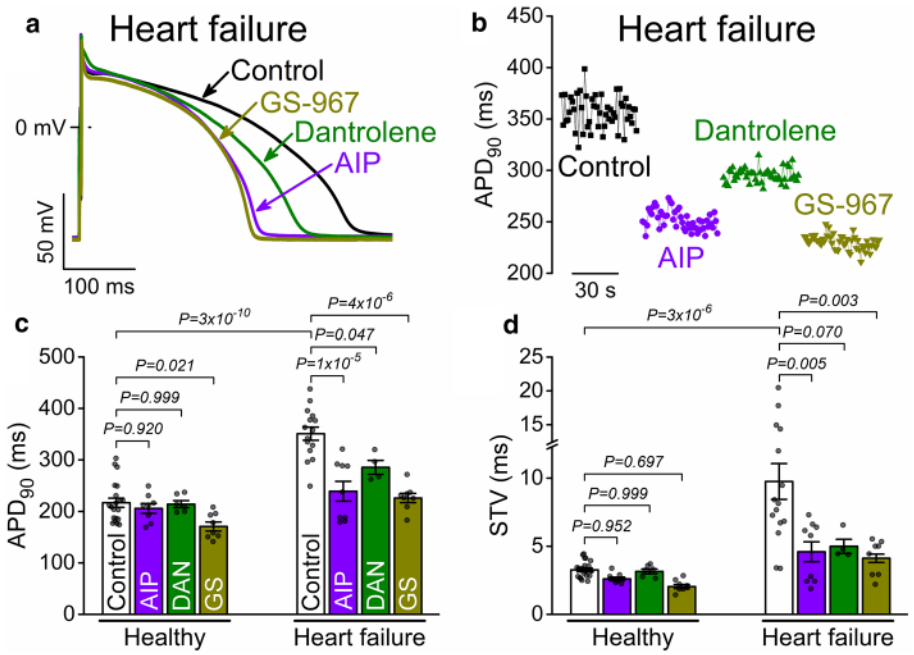

Fig. 2 CaMKII, leaky RyRs, and late Na^+ current promote arrhythmogenic AP changes in HF. **a** Representative APs in failing rabbit ventricular myocytes in control and following treatments with either the selective CaMKII inhibitor AIP (1 µmol/L), the pathological RyR conformation inhibitor dantrolene (DAN, 10 µmol/L) or the late Na^+ current inhibitor GS-967 (GS, 1 µmol/L) **b** 50 consecutive AP durations at 90% repolarization (APD_{90}). **c** APD_{90} in age-matched healthy and failing rabbit cardiomyocytes. ANOVA with Dunnett's multiple comparisons test. **d** Short-term variability (STV) of APD_{90}. Cells were paced at 1 Hz. ANOVA with Dunnett's multiple comparisons test. ($N = 10$ HF and 10 age-matched control rabbits, each individual myocyte (n) is shown as a data point.)

change (Fig. 4a, c); however, STV was markedly increased (Fig. 4b, d). Importantly, the I_{NaL} inhibitor GS-967 (and not a direct SR Ca^{2+} leak modulator) significantly shortened APD_{90} following caffeine + ISO and attenuated the increase in STV (Fig. 4a–d). Cell pretreatment with the mitochondrial ROS (mitoROS) scavenger mitoTEMPOL (20 µmol/L) or AIP did not change significantly baseline APD_{90} and STV (Fig. 4c, d). However, caffeine + ISO induced APD_{90} shortening in both mitoTEMPOL and AIP pretreated cells (Fig. 4a–d). The additional application of GS-967 no longer altered APD_{90} in mitoTEMPOL and AIP pretreated cells (Fig. 4a–d). These data indicate that mitoROS-CaMKII signalling markedly upregulates I_{NaL} following RyR leak enhancement and contributes to increased beat-to-beat APD_{90}-variability. Thus, SR Ca^{2+} leak enhancement recruits ROS, I_{NaL} and CaMKII as part of its integrated response.

RyR leak-induced DADs are suppressed by synergistic inhibition of I_{NaL}, mitoROS and CaMKII

Because RyR leak is associated with the development of arrhythmogenic delayed afterdepolarizations (DADs), we tested the contribution of enhanced I_{NaL}-mitoROS-CaMKII feedback to DAD occurrence. Caffeine + ISO induced spontaneous SR Ca^{2+} release (sCaR) events between paced beats in myocytes loaded with the intra-SR ($[Ca^{2+}]_{SR}$) fluorescent indicator, Mag-Fluo-4 (Fig. 5a, b). In parallel current-clamp experiments, caffeine + ISO also induced DADs with a frequency of 35 ± 5/min and amplitude of 5.1 ± 0.2 mV during steady-state pacing (Fig. 5c–e). Following GS-967 treatment, the frequency of sCaRs (Fig. 5b) and DADs (Fig. 5d) was unchanged, but GS-967 significantly reduced the DAD amplitude (Fig. 5e), especially the large DADs (Fig. 5f). Importantly, DAD frequency was significantly reduced in cells preincubated with either mitoTEMPOL or AIP (7 ± 3/min and 9 ± 4/min, respectively; Fig. 5d). MitoTEMPOL and AIP also significantly increased DAD latency upon caffeine + ISO treatment (Fig. 5g). Moreover, cumulative application of GS-967 tended to further reduce DAD frequency in mitoTEMPOL and AIP pretreated cells (2 ± 1/min in both cases; Fig. 5d).

Next, we examined the stability of the SR Ca^{2+} release system following cessation of pacing. Caffeine + ISO induced spontaneous SR Ca^{2+} release events, which were attenuated in mitoTEMPOL-treated cells (Fig. 6a, b). Caffeine + ISO induced multiple DADs and, in a few instances, spontaneous APs (sAPs) following cessation of tachypacing (Fig. 6c). The frequency of DADs was markedly attenuated by cell pretreatment with mitoTEMPOL or AIP (Fig. 6d). Addition of GS-967 reduced DAD frequency only

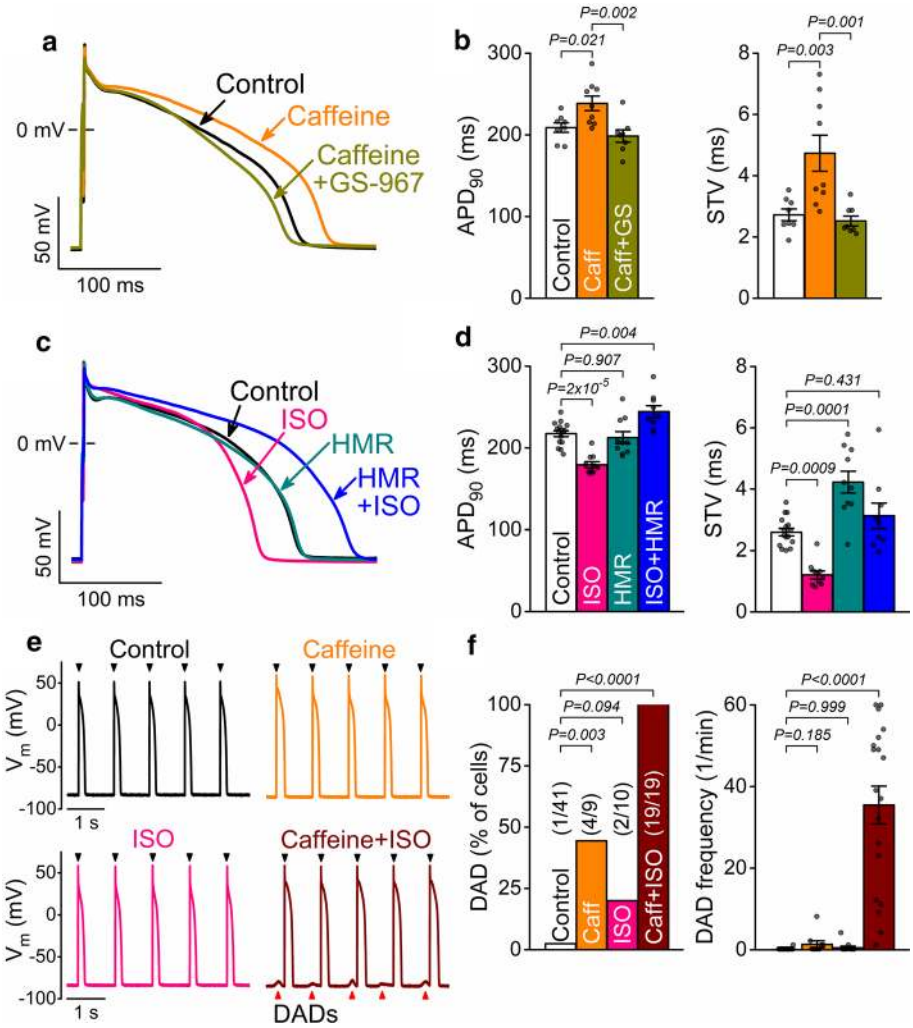

Fig. 3 Caffeine and isoproterenol induced AP changes in healthy rabbit ventricular myocytes. **a** Representative rabbit ventricular APs in control and low-dose caffeine (Caff, 200 µmol/L), and after application of the late Na^+ current inhibitor GS-967 (GS, 1 µmol/L). **b** APD_{90} and STV were increased by Caff, then restored by GS. **c** Representative APs in control and following β-adrenergic agonist isoproterenol (ISO, 100 nmol/L) stimulation, and after application of the slow delayed rectifier K^+ current inhibitor HMR-1556 (HMR, 1 µmol/L). **d** APD_{90} and its short-term variability (STV) in control, ISO, HMR, and ISO + HMR. **e** APs and delayed afterdepolarizations (DADs, indicated by red arrowheads) following combined treatment with Caff + ISO at 1 Hz steady-state pacing. **f** Percent of cells showing DADs and the frequency of DADs during 1 Hz pacing for 1 min. APD_{90} and STV were compared using ANOVA with Tukey's multiple comparisons test. Number of cells showing DADs was compared using Fisher's exact test. DAD frequencies were compared using Kruskal–Wallis ANOVA with Dunn's multiple comparisons test. ($N = 5$–17 animals in each treatment group, each individual myocyte (n) is shown as a data point.)

in MitoTEMPOL-pretreated cells but did not change DAD amplitude following cessation of pacing (Fig. 6e).

These data indicate that mitochondrial superoxide production and CaMKII activation markedly enhance DADs in cells with pronounced RyR leak, and a combined treatment of mitoTEMPOL or AIP and GS-967 is largely protective against DADs.

Enhanced I_{NaL} induces RyR leak that further prolongs APD

Next, we tested whether proarrhythmic AP changes induced by enhanced I_{NaL} are attenuated by dantrolene in healthy rabbit ventricular myocytes. Anemone toxin II (ATX-II, 5 nmol/L) significantly enhanced I_{NaL} during AP-clamp, and the net charge carried by I_{NaL} increased by 3.9-fold (Fig. 7a, b). In current-clamp, ATX-II also prolonged APD_{90} (mimicking LQT3) and markedly increased STV (Fig. 7c, d). Importantly, dantrolene attenuated the ATX-II-induced

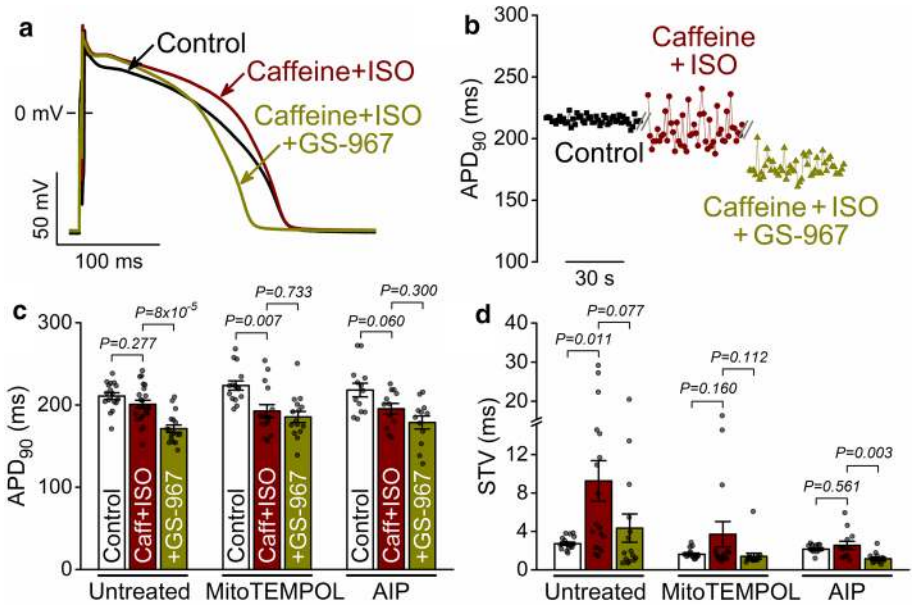

Fig. 4 RyR leak enhances late Na^+ current, mito-ROS and CaMKII to induce proarrhythmic AP changes. **a** Representative rabbit ventricular APs in control and following caffeine (Caff, 200 µmol/L) and isoproterenol (ISO, 100 nmol/L) stimulation, and after application of the late Na^+ current inhibitor GS-967 (1 µmol/L). **b** Fifty consecutive APD_{90} over time demonstrating increased APD_{90}-variability following application of caffeine and isoproterenol. **c** APD_{90} in cells without pretreatment and following pretreatment with MitoTEMPOL (20 µmol/L) and CaMKII inhibitor AIP (1 µmol/L). **d** Short-term variability (STV) of APD_{90}. ANOVA with Tukey's multiple comparisons test. ($N = 6$–10 animals in each treatment group, each individual myocyte (n) is shown as a data point.)

APD prolongation (Fig. 7c), and this dantrolene effect was absent in cells preincubated with mitoTEMPOL and AIP (Fig. 7e). Moreover, mitoTEMPOL and AIP slightly reduced the increase in STV by ATX-II (Fig. 7f). These data indicate that the mitoROS-CaMKII-induced RyR leak contributes to APD prolongation when I_{NaL} is enhanced by ATX-II. However, the dantrolene impact on APD prolongation is modest.

I_{NaL} induced EADs are attenuated by dantrolene, mitoTEMPOL and AIP

ATX-II also increased systolic and diastolic intracellular Ca^{2+} levels (measured as change in Rhod-2 fluorescence) and prolonged the $[Ca^{2+}]_i$ transient (CaT, Fig. 8a). ATX-II markedly prolonged APD at low pacing rates (Fig. 8b) and 10 nmol/L ATX-II induced early afterdepolarizations (EADs) (Fig. 8c). Dantrolene slightly attenuated both the frequency and amplitude of EADs in ATX-II (Fig. 8c–f). Interestingly, mitoTEMPOL preincubation markedly reduced the frequency (Fig. 8d) but not the amplitude of the EADs (Fig. 8e); however, mitoTEMPOL delayed the time to the first EAD significantly (Fig. 8g). In contrast to mitoTEMPOL, AIP was only slightly protective against EAD formation induced by ATX-II (Fig. 8d). These data indicate that ROS production, and also slightly CaMKII and RyR leak contribute to ATX-II induced EADs.

Dantrolene reduces arrhythmogenic activities in SCN5A N406K hiPSC-CMs

Next, we tested the effects of dantrolene in hiPSC-CMs carrying the SCN5A N406K LQT3 mutation, which has been associated with significant QT prolongation, increased risk of torsade de pointes-type ventricular tachycardia and sudden cardiac death [60]. Previous biophysical characterization [31] showed that the mutant channels exhibit an interesting mixed phenotype with increased I_{NaL} as gain-of-function (long QT3) and a decreased peak I_{Na} (due to reduced surface expression of Na^+ channels) as loss-of-function (Brugada syndrome). Importantly, these changes in Na^+ channel function are similar to the CaMKII-mediated effects [67] and remodelling in HF [65]. Moreover, hiPSC-CMs carrying the SCN5A N406K mutation also showed impaired intracellular Ca^{2+} handling and Ca^{2+}-dependent arrhythmias [60].

APs in SCN5A N406K and wild type (WT) hiPSC-CMs, cultured in a metabolic maturation media and paced at 1 Hz [12], exhibited sufficiently negative diastolic V_m to enable robust Na^+ channel availability and AP rate of rise (Fig. 9a–c). Even so the N406K vs. WT cells exhibited lower maximal upstroke velocity (dV/dt_{max}), prolonged APD_{90}, and significant AP triangulation, in line with data in literature and the expected consequences of decreased peak I_{Na} and increased I_{NaL} (Fig. 9a–c). Cells carrying the N406K mutation also had frequent spontaneous depolarizations (Fig. 9b).

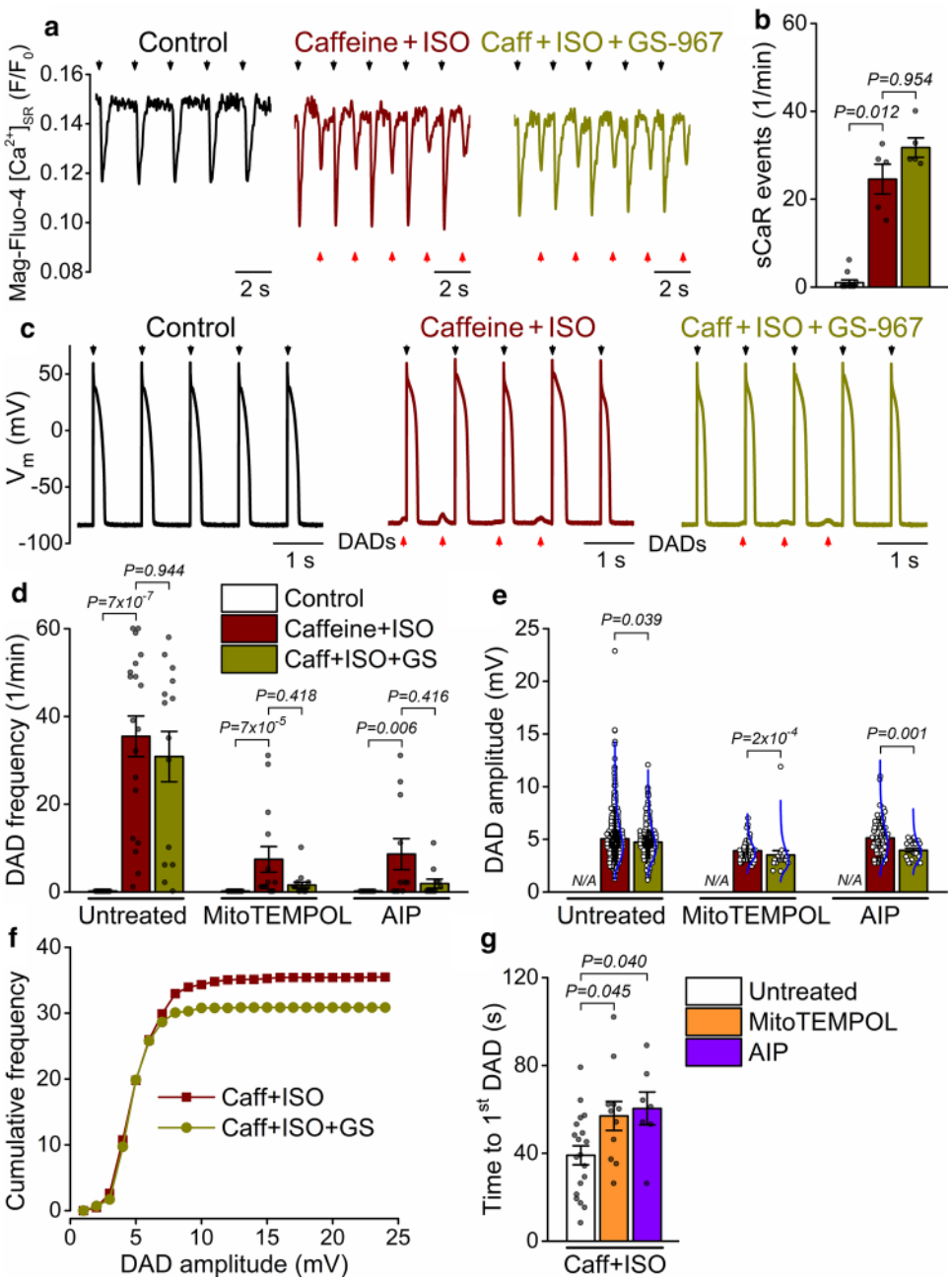

Fig. 5 RyR leak synergizes with mito-ROS, CaMKII, and late Na^+ current to promote DADs. **a** Sarcoplasmic reticulum Ca^{2+} release (monitored as Mag-Fluo-4 fluorescence) in control and following caffeine (Caff, 200 µmol/L) and isoproterenol (ISO, 100 nmol/L) stimulation, and after application of GS-967 (GS, 1 µmol/L). Rabbit ventricular cells were paced at 0.5 Hz steady state. Black arrowheads indicate pacing signals, and red arrowheads indicate spontaneous Ca^{2+} release (sCaR) events. **b** Frequency of sCaR events. **c** APs and delayed afterdepolarizations (DADs, indicated by red arrowheads) at 1 Hz steady-state pacing. **d** DAD frequency during 1 Hz pacing for 1 min in cells without pretreatment and following pretreatment with MitoTEMPOL (20 µmol/L) and CaMKII inhibitor AIP (1 µmol/L). **e** DAD amplitude. Blue lines represent lognormal distribution curves. **f** Cumulative DAD frequencies as a function of DAD amplitudes. **g** Time to first DAD after application of caff + ISO. Cells were paced at 1 Hz steady-state. DAD and sCaR frequencies were compared using Kruskal–Wallis ANOVA with Dunn's multiple comparisons test; DAD amplitudes were compared using Mann–Whitney test. ($N = 6$–9 animals in each treatment group, each individual myocyte (n) is shown as a data point.)

Moreover, significant APD alternans occurred in N406K mutants at higher pacing rates (starting at 3 Hz; Fig. 9b). Importantly, dantrolene treatment significantly reduced the spontaneous depolarizations and shortened APD_{90} in N406K, while it had no effect on APD_{90} in WT hiPSC-CMs (Fig. 9a–c). Dantrolene also increased the APD alternans threshold frequency (from 3 to 4 Hz) and reduced the amplitude of APD alternans (Fig. 9c). These data reinforce the suggested interplay between I_{NaL} and RyR in the vicious cycle.

Discussion

Impairments in cardiomyocyte Na^+ and Ca^{2+} handling are characteristic of HF and contribute to contractile dysfunction and arrhythmias [45, 54, 68]. In our HF rabbit model, $[Na^+]_i$ was found to be 3 mmol/L higher than in control [8]. In agreement with this, I_{NaL} was increased by 82% in failing rabbit myocytes, and the I_{NaL} upregulation was predominantly CaMKII-dependent [27]. CaMKIIδ_C expression and autophosphorylation were increased by 112% and 260%, respectively, in HF rabbit hearts, and similar increases were found in human heart samples from patients with dilated and

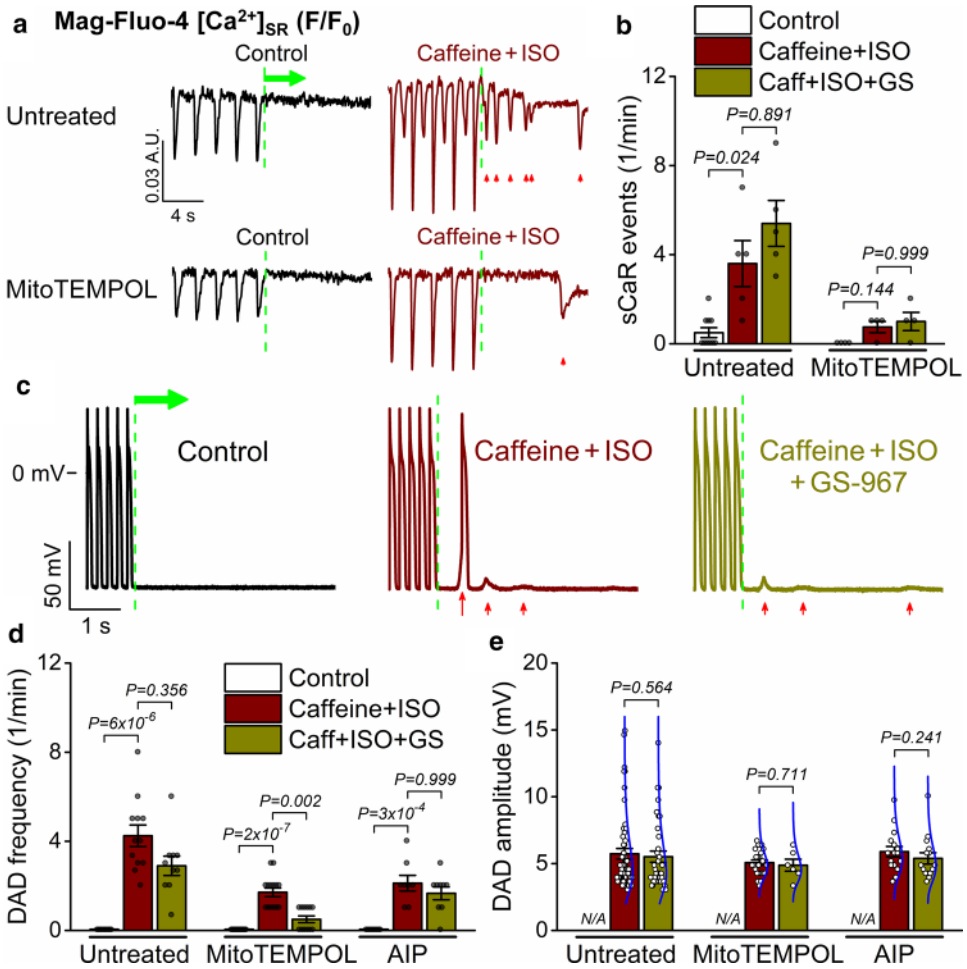

Fig. 6 Mito-ROS, CaMKII and late Na^+ current promote spontaneous diastolic activities. **a** Spontaneous SR Ca^{2+} release (sCaR) events following cessation of pacing (indicated by green dashed lines) were induced by caffeine (Caff, 200 µmol/L) and isoproterenol (ISO, 100 nmol/L) stimulation. Pretreatment with MitoTEMPOL (20 µmol/L) attenuated the sCaR events. Rabbit ventricular myocytes were loaded with Mag-Fluo-4AM. **b** Frequency of sCaR events. **c** Delayed afterdepolarizations (DADs) following cessation of tachypacing (5 Hz), which elicited spontaneous APs in some instances. **d**, **e** DAD frequency and amplitude during a 1-min recording following cessation of tachypacing. Late Na^+ current was inhibited using GS-967 (GS, 1 µmol/L), and CaMKII was inhibited using AIP (1 µmol/L). Blue lines represent lognormal distribution curves. DAD and sCaR frequencies were compared using Kruskal–Wallis one-way ANOVA with Dunn's multiple comparisons test; DAD amplitudes were compared using Mann–Whitney test. ($N = 6$–7 animals in each treatment group, each individual myocyte (n) is shown as a data point.)

ischemic cardiomyopathies [5]. CaMKII-dependent phosphorylation of RyR2 at S2814 was increased by 105% in rabbit HF [1] and led to increased SR Ca^{2+} leak at a given SR Ca^{2+} load [58]. Moreover, NCX expression and NCX current were also increased by 93% and 120%, respectively, in HF rabbits [53]. Furthermore, the membrane resistance is increased in HF due to 25–50% reduction in inward rectifier K^+ current (I_{K1}) [22, 54], thus, a given depolarizing current can cause larger DADs. The magnitude of I_{K1} reduction quantitatively matches the downregulation of Kcnj2/$K_{ir}2.1$ expression upon chronic CaMKII overexpression [21]. Taken together, less $\Delta[Ca^{2+}]_i$ is required to trigger a spontaneous AP in failing cardiomyocytes [54]. Importantly, CaMKII inhibition was shown to prevent DADs in isolated failing cardiomyocytes [22] and reduced in vivo arrhythmia inducibility in HF [28]. Calcium- and CaMKII dependent arrhythmias were also demonstrated in long QT caused by either gain-of-function mutation in Na^+ channels [72] or loss-of-function mutation in K^+ channels [63]. Along the same lines, in RyR-mutant CPVT, inhibition of CaMKII markedly attenuated proarrhythmic activities [4, 38]. These data indicate the activation of the vicious cycle and its pivotal role in arrhythmogenesis in HF, LQT, and CPVT.

ROS is a critical mediator of pathological cellular remodelling and contributes to impaired cardiomyocyte Na^+ and Ca^{2+} homeostasis in heart diseases [15]. Our data support the concept of a strong, bidirectional feedback between SR Ca^{2+} leak and increased ROS [17]. ROS can oxidize RyRs

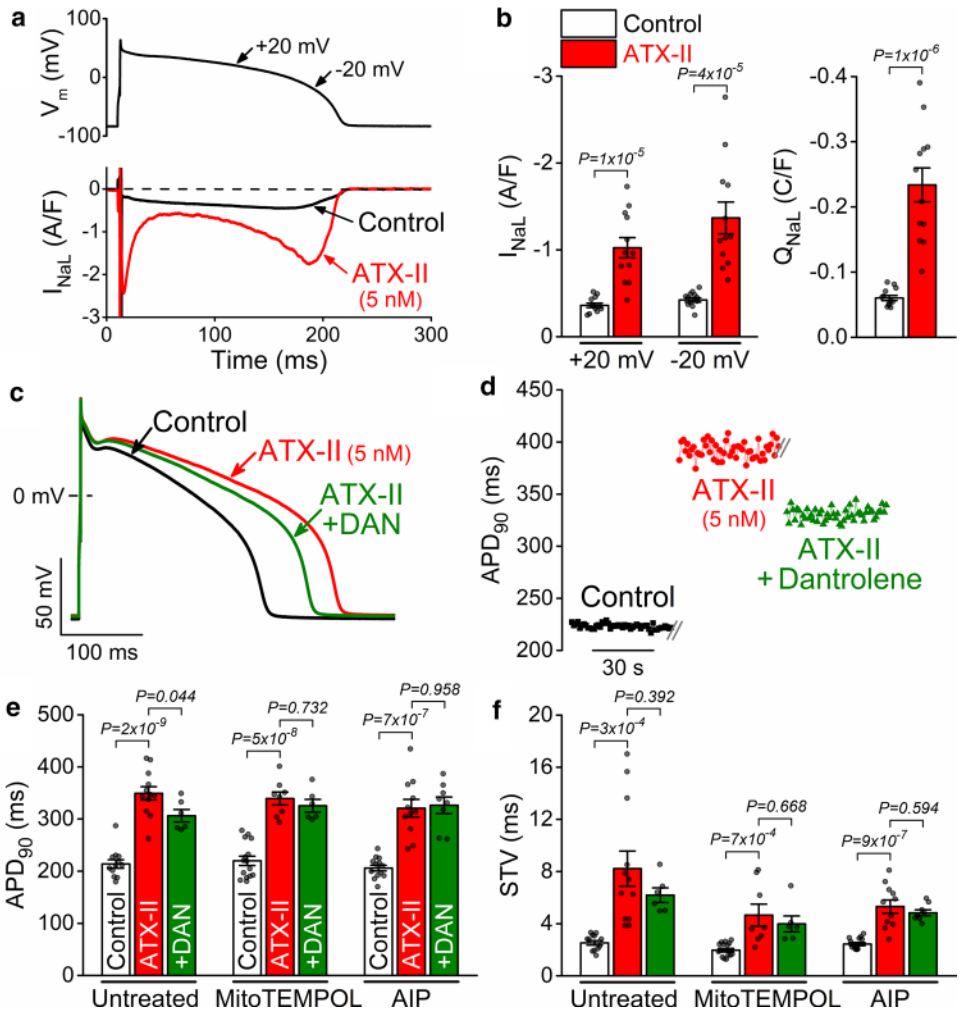

Fig. 7 Dantrolene attenuates APD prolongation induced by enhanced late Na^+ current. **a** Late Na^+ current (I_{NaL}) in AP-clamped rabbit ventricular myocytes in control and following ATX-II (5 nmol/L). **b** I_{NaL} density at + 20 mV and − 20 mV, and net charge (Q_{NaL}) carried by I_{NaL} under AP-clamp. Student's *t*-test. **c** Representative rabbit ventricular APs in control and in the presence of ATX-II, and after application of dantrolene (DAN, 10 µmol/L). **d** Increased APD_{90}-variability following ATX-II. **e** APD_{90} in cells without pretreatment and following pretreatment with MitoTEMPOL (20 µmol/L) and CaMKII inhibitor AIP (1 µmol/L). **f** Short-term variability (STV) of APD_{90}. ANOVA with Tukey's multiple comparisons test. ($N = 5–7$ animals in each treatment group, each individual myocyte (n) is shown as a data point.)

[50] and induce autonomous CaMKII activation [11], both further increase SR Ca^{2+} leak [62, 69]. SR Ca^{2+} leak then may increase Ca^{2+} uptake into neighbouring mitochondria via the mitochondrial Ca^{2+} uniporter (MCU) [3, 36]. Oxidation of MCU can also increase its activity [10]. Furthermore, CaMKII can also increase ROS via NADPH oxidase 2 (NOX2) [41, 49]. While some data in isolated mitochondria suggested elevated mitochondrial [Ca^{2+}] in HF (due to leaky RyRs and increased mitochondrial Ca^{2+} uptake [57]), more direct HF measurements in intact guinea-pig ventricular myocytes indicated reduced mitochondrial [Ca^{2+}] (due to elevated $[Na^+]_i$, lower CaTs and greater Ca^{2+} extrusion via mitochondrial Na^+/Ca^{2+} exchange) [42]. Moreover, both increased and decreased mitochondrial [Ca^{2+}] may increase ROS production [7]. Interestingly, a recent paper showed that moderate overexpression of MCU that enhances mitochondrial Ca^{2+} uptake also improves HF phenotype by reducing SR Ca^{2+} leak [40]. This highlights the pathophysiological role of the vicious cycle and mitochondrial ROS therein.

Ion channel remodelling in HF leads to APD prolongation and increased STV [22], creating a vulnerable arrhythmia substrate. APD prolongation then may promote further cellular Na^+ and Ca^{2+} loading and CaMKII activation (Fig. 1). Inhibition of the upregulated I_{NaL}, CaMKII and leaky RyRs all reduced APD prolongation and STV in HF (Fig. 2). In contrast, acute pharmacological induction of RyR leak by caffeine + isoproterenol did not change APD (Fig. 4). The more pronounced APD change by RyR leak in HF cardiomyocytes might reflect the effect of reduced repolarization reserve (downregulated K^+ channels [46]) and altered balance between inward and outward ionic currents [23, 24]. In line with this, inhibition of I_{Ks} led to APD prolongation following β-adrenergic stimulation in rabbit (Fig. 3) and human [33] ventricular myocytes. Hamilton et al. [18] also showed that caffeine + isoproterenol but not isoproterenol alone increased mitoROS production. Moreover, we have shown a two-hit arrhythmia model in which hyperglycaemia-induced CaMKII activation and RyR leak alone did not change APD, but when repolarization reserve was reduced, a marked APD prolongation occurred [26]. Like with

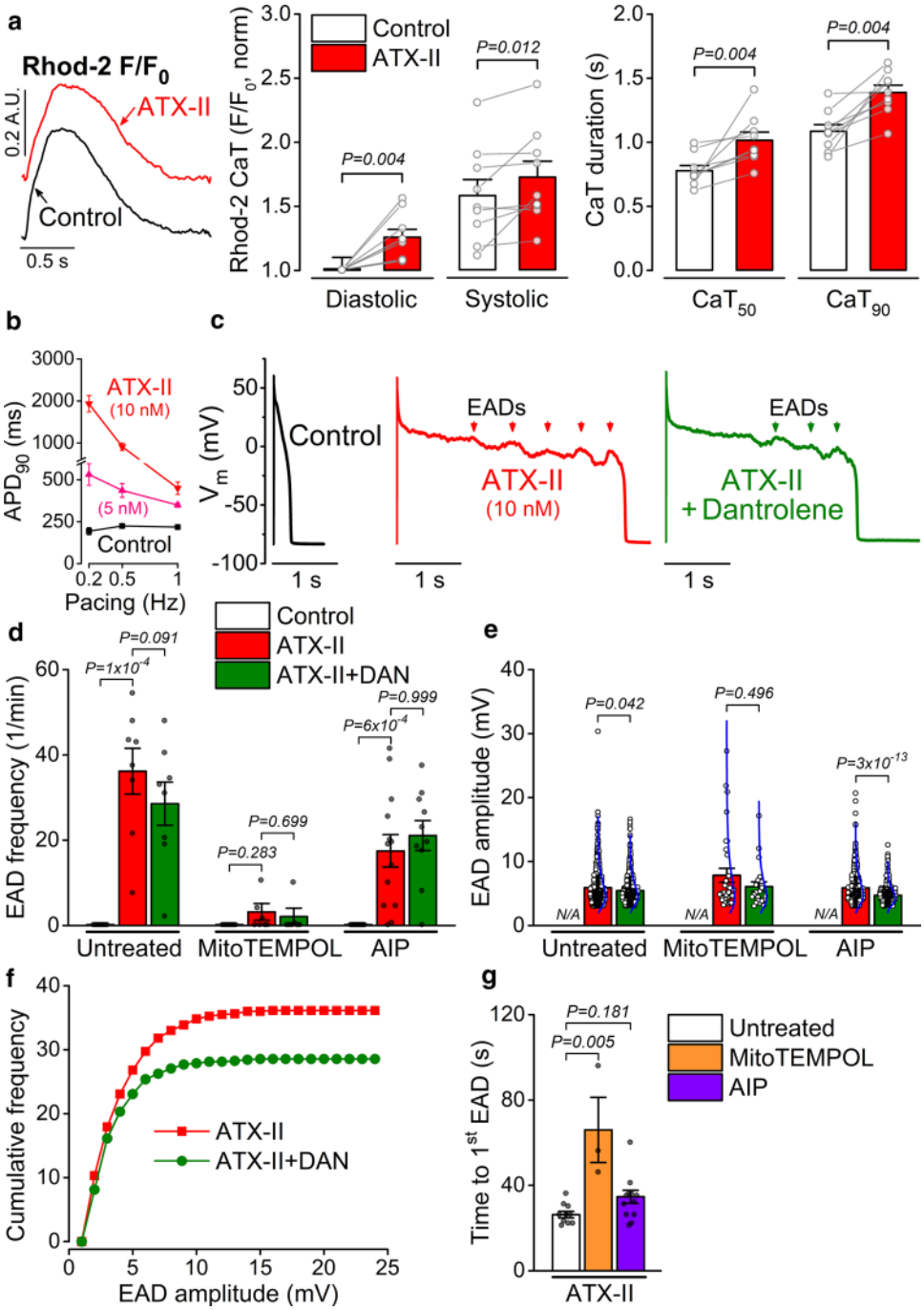

Fig. 8 Enhanced late Na^+ current induces RyR leak, mito-ROS and CaMKII to promote EADs. **a** Intracellular Ca^{2+} transient (CaT) measured as Rhod-2 fluorescence in control and ATX-II (10 nmol/L) in rabbit ventricular myocytes paced at 0.5 Hz. The error bar on the control diastolic value indicates the degree of variability in the baseline raw F (F/non-cellular background), and F_0 is the control baseline F in each cell. Wilcoxon matched-pairs signed rank test. **b** Reverse-rate dependent APD_{90} prolongation by ATX-II (5 and 10 nmol/L). **c** Early afterdepolarizations (EADs, red arrowheads) at 0.2 Hz steady-state pacing in a representative rabbit ventricular cell in control and ATX-II (10 nmol/L), and after application of dantrolene (DAN, 10 µmol/L). **d**, **e** EAD frequency and amplitude during pacing in cells without pretreatment and following pretreatment with MitoTEMPOL (20 µmol/L) and CaMKII inhibitor AIP (1 µmol/L). Blue lines represent lognormal distribution curves. **f** Cumulative EAD frequencies as a function of EAD amplitudes. **g** Time to first EAD after application of ATX-II. Cells were paced at 0.2 Hz steady-state. EAD frequencies were compared using Friedman repeated measure ANOVA with Dunn's multiple comparisons test. EAD amplitudes were compared using Mann–Whitney test. ($N = 3$–7 animals in each treatment group, each individual myocyte (n) is shown as a data point.)

arrhythmia induction, arrhythmia termination may require two simultaneous targets. Such synergy was observed when either MitoTEMPOL or AIP was combined with GS-967 leading to a marked reduction in DADs (Figs. 5, 6). Then, in an inverse experimental setting, enhanced I_{NaL} prolonged APD (Fig. 7), increased $[Ca^{2+}]_i$, and induced EADs (Fig. 8). Multiple mechanisms can contribute to EADs, including spontaneous SR Ca^{2+} release and inward NCX, reopening of L-type Ca^{2+} channels (LTCC), and augmentation of I_{NaL}, and all of these are modulated by $[Ca^{2+}]_i$ and CaMKII [30, 55]. CaMKII inhibition attenuated EADs (Fig. 8) and buffering $[Ca^{2+}]_i$ has been previously shown to abolish EADs induced by ATX-II [29]. Experimental [71] and computational modelling [13] studies mechanistically investigated the EAD mechanisms upon H_2O_2 treatment and showed that EADs emerge at slow pacing rates upon simultaneous activation of both LTCC and Na^+ channels via ROS-dependent CaMKII activation (and alone, neither RyR nor I_{NaL} nor LTCC effects were sufficient to produce EADs). Intracellular Na^+ loading induced by either ouabain [39] or ATX-II

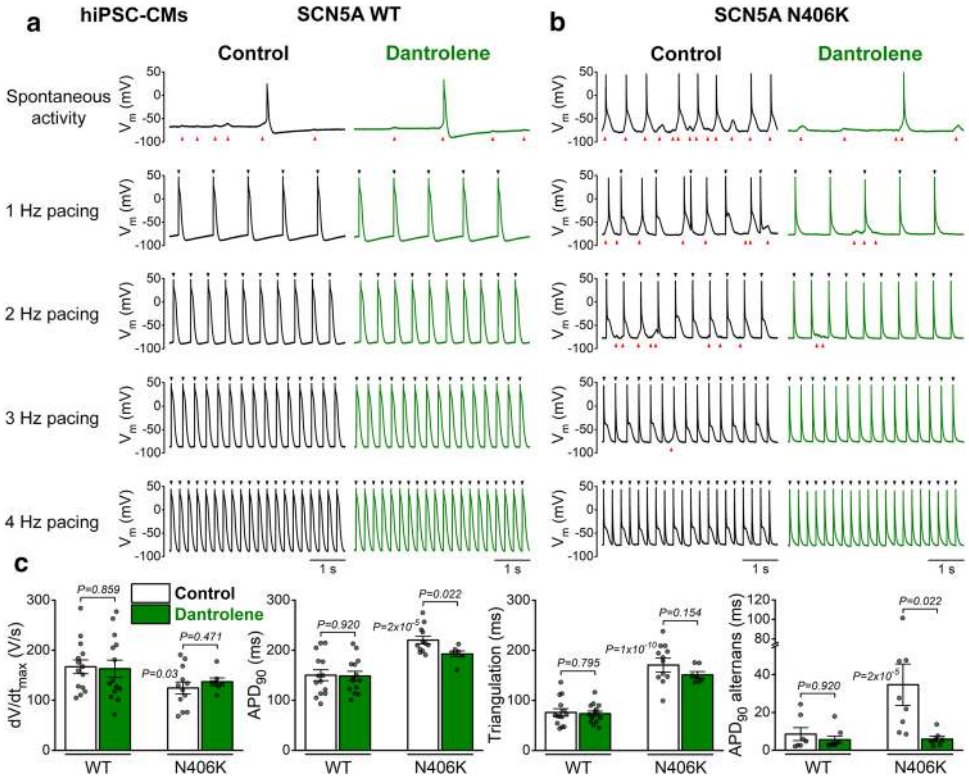

Fig. 9 Dantrolene reduces arrhythmogenic activities in SCN5A N406K hiPSC-CMs. **a** Series of action potentials (APs) without pacing and using increasing pacing frequencies from 1 to 4 Hz in control and following dantrolene (10 µmol/L) treatment in a representative wild-type (WT) hiPSC-CM. Black arrowheads on top of each trace indicate pacing signals. Red arrowheads at the bottom of each trace indicate spontaneous depolarizations. **b** Representative APs in control and following dantrolene treatment in SCN5A N406K hiPSC-CM. **c** Summary data on maximal upstroke velocity (dV/dt_{max}), AP duration at 90% repolarization (APD_{90}), AP triangulation (APD_{90}–APD_{50}) at 1 Hz pacing, and the magnitude of APD_{90} alternans in subsequent beats at 4 Hz pacing. Student's paired *t*-test and ANOVA with Tukey's multiple comparisons test. (Each individual hiPSC-CM (*n*) is shown as a data point.)

[34, 66] treatment has been shown to increase mitoROS and diastolic Ca^{2+}-triggered arrhythmias. Here we showed that mitoROS also plays an important role in mediating EADs induced by the ATX-II-enhanced I_{NaL} (Fig. 8), which may reflect spatial and functional coupling between $Na_V1.5$ channels and mitochondria [52]. Moreover, multiscale modelling of the mitochondria-SR microdomain showed that elevated ROS production increases $[Ca^{2+}]_i$ and arrhythmia propensity by stimulating RyRs and inhibiting SERCA [37]. Consistent with this, MitoTEMPOL pretreatment significantly prolonged EAD latency (Fig. 8) suggesting that the increase in ROS is an early response to $[Na^+]_i$ loading. Interestingly, inhibition of SR Ca^{2+} leak by dantrolene attenuated APD prolongation following ATX-II treatment (Fig. 7) and in HF (Fig. 2). The effects of dantrolene on APD (and EAD formation) might be explained by the attenuation of SR Ca^{2+} leak-induced CaMKII activity, changes in myocyte Na^+ and Ca^{2+} loading, enhanced inward NCX, and late Ca^{2+} sparks, which can activate the vicious cycle and influence AP configuration [14]. Dantrolene also markedly attenuated APD prolongation, alternans, and spontaneous diastolic activities (i.e., DADs, sAPs) in hiPSC-CMs carrying SCN5A N406K mutation, highlighting the critical role of SR Ca^{2+} leak (and the activated vicious cycle) in these arrhythmias (Fig. 9).

Here, we aimed to preserve physiological regulation in our cellular experiments to uncover interactions within the feedback loops. However, this approach has limitations on quantifying the exact role that each component plays in the vicious cycle. Full inhibition of one key component may break the whole loop and have a marked arrhythmia reducing effect, like that seen in HF (Fig. 2). However, this approach may overestimate the individual contribution of one arm in the feedback loop. On the contrary, the APD shortening effect of dantrolene in HF (Fig. 2), ATX-II-induced long QT3 (Fig. 7), and SCN5A N406K (Fig. 9), and the antiarrhythmic effects of MitoTEMPOL and AIP in pharmacologically enhanced I_{NaL} (Fig. 5) and RyR leak (Fig. 8) clearly demonstrate the importance and strength of the vicious cycle. The interaction between $[Na^+]_i$ loading and ROS in promoting arrhythmias was found to be particularly strong, which then can lead to further RyR leak and CaMKII activation. In line with this, such synergy between

multiple antiarrhythmic targets (e.g., inhibition of both Na^+ channels and leaky RyRs) may contribute to the clinical benefit of flecainide [35] and ranolazine [51]. Future, mechanistic experiments (e.g., using permeabilized myocytes) could determine the quantitative relationship between $[Na^+]_i$ and mitochondrial ROS production at a given $[Ca^{2+}]_i$. Incorporating these data may help to constrain and improve computational models in the future, which then would allow more controlled analysis of different branches of the vicious cycle.

As discussed above, many components of the $[Na^+]_i$–$[Ca^{2+}]_i$–ROS-CaMKII-RyR leak vicious cycle signalling have already been shown; however, the strength of feedback interactions have not been previously investigated. Our conceptual novelty here is the identification of important *trans*-target effects beyond the *on*-target effects of the otherwise selective inhibitors. It may have important clinical implications suggesting that potentially a combination therapy targeting the major components of the arrhythmogenic vicious cycle described here can be synergistic and may provide substantial benefits in heart diseases by reducing cellular proarrhythmia. The use of combination therapy may also be advantageous by reducing the effective dose of each drug, thus reducing their adverse effects. Moreover, our data show that the most favourable drug target(s) may vary among heart diseases, and thus, personalized medicine approaches are required to identify the optimal drug combinations.

Acknowledgements We thank Nima R. Habibi, Benjamin W. Van, Erin Y. Shen, Sonya Baidar, and Maura Ferrero for their help in animal care, cell isolation, and laboratory tasks. We also thank Dr. William T. Ferrier, Linda Talken, and Lynette M. Mendoza for their help in surgical procedures and echocardiographic follow-up of HF rabbits. We also thank Francesca Briganti and members of the Mercola laboratory for providing hiPSC-CM lines.

Funding This work was supported by grants from the National Institutes of Health (NIH) P01-141084 to DMB and MM, and R01-142282 to DMB and JB, the Finnish Cultural Foundation 00200088 to RPP, and the Osk. Huttunen Foundation to RPP.

Availability of data and materials All data and materials are available on reasonable request to the corresponding author.

Declarations

Conflict of interest The authors declare that they have no conflict of interest.

Ethical approval All animal handling and laboratory procedures were in accordance with the approved protocols (#21572 and #21137) of the Institutional Animal Care and Use Committee at University of California, Davis conforming to the NIH Guide for the Care and Use of Laboratory Animals (8th edition, 2011).

References

1. Ai X, Curran JW, Shannon TR, Bers DM, Pogwizd SM (2005) Ca^{2+}/calmodulin-dependent protein kinase modulates cardiac ryanodine receptor phosphorylation and sarcoplasmic reticulum Ca^{2+} leak in heart failure. Circ Res 97:1314–1322. https://doi.org/10.1161/01.RES.0000194329.41863.89
2. Bers DM (2008) Calcium cycling and signaling in cardiac myocytes. Annu Rev Physiol 70:23–49. https://doi.org/10.1146/annurev.physiol.70.113006.10045
3. Bertero E, Maack C (2018) Calcium signaling and reactive oxygen species in mitochondria. Circ Res 122:1460–1478. https://doi.org/10.1161/CIRCRESAHA.118.310082
4. Bezzerides VJ, Caballero A, Wang S, Ai Y, Hylind RJ, Lu F, Heims-Waldron DA, Chambers KD, Zhang D, Abrams DJ, Pu WT (2019) Gene therapy for catecholaminergic polymorphic ventricular tachycardia by inhibition of Ca^{2+}/calmodulin-dependent kinase II. Circulation 140:405–419. https://doi.org/10.1161/CIRCULATIONAHA.118.038514
5. Bossuyt J, Helmstadter K, Wu X, Clements-Jewery H, Haworth RS, Avkiran M, Martin JL, Pogwizd SM, Bers DM (2008) Ca^{2+}/calmodulin-dependent protein kinase IIdelta and protein kinase D overexpression reinforce the histone deacetylase 5 redistribution in heart failure. Circ Res 102:695–702. https://doi.org/10.1161/CIRCRESAHA.107.169755
6. Coppini R, Santini L, Olivotto I, Ackerman MJ, Cerbai E (2020) Abnormalities in sodium current and calcium homoeostasis as drivers of arrhythmogenesis in hypertrophic cardiomyopathy. Cardiovasc Res 116:1585–1599. https://doi.org/10.1093/cvr/cvaa124
7. Cortassa S, Juhaszova M, Aon MA, Zorov DB, Sollott SJ (2021) Mitochondrial Ca^{2+}, redox environment and ROS emission in heart failure: two sides of the same coin? J Mol Cell Cardiol 151:113–125. https://doi.org/10.1016/j.yjmcc.2020.11.013
8. Despa S, Islam MA, Weber CR, Pogwizd SM, Bers DM (2002) Intracellular Na^+ concentration is elevated in heart failure but Na/K pump function is unchanged. Circulation 105:2543–2548. https://doi.org/10.1161/01.cir.0000016701.85760.97
9. Dey S, DeMazumder D, Sidor A, Foster DB, O'Rourke B (2018) Mitochondrial ROS drive sudden cardiac death and chronic proteome remodeling in heart failure. Circ Res 123:356–371. https://doi.org/10.1161/CIRCRESAHA.118.312708
10. Dong Z, Shanmughapriya S, Tomar D, Siddiqui N, Lynch S, Nemani N, Breves SL, Zhang X, Tripathi A, Palaniappan P, Riitano MF, Worth AM, Seelam A, Carvalho E, Subbiah R, Jana F, Soboloff J, Peng Y, Cheung JY, Joseph SK, Caplan J, Rajan S, Stathopulos PB, Madesh M (2017) Mitochondrial Ca^{2+} uniporter is a mitochondrial luminal redox sensor that augments MCU channel activity. Mol Cell 65:1014–1028. https://doi.org/10.1016/j.molcel.2017.01.032

11. Erickson JR, Joiner ML, Guan X, Kutschke W, Yang J, Oddis CV, Bartlett RK, Lowe JS, O'Donnell SE, Aykin-Burns N, Zimmerman MC, Zimmerman K, Ham AJ, Weiss RM, Spitz DR, Shea MA, Colbran RJ, Mohler PJ, Anderson ME (2008) A dynamic pathway for calcium-independent activation of CaMKII by methionine oxidation. Cell 133:462–474. https://doi.org/10.1016/j.cell.2008.02.048
12. Feyen DAM, McKeithan WL, Bruyneel AAN, Spiering S, Hormann L, Ulmer B, Zhang H, Briganti F, Schweizer M, Hegyi B, Liao Z, Polonen RP, Ginsburg KS, Lam CK, Serrano R, Wahlquist C, Kreymerman A, Vu M, Amatya PL, Behrens CS, Ranjbarvaziri S, Maas RGC, Greenhaw M, Bernstein D, Wu JC, Bers DM, Eschenhagen T, Metallo CM, Mercola M (2020) Metabolic maturation media improve physiological function of human iPSC-derived cardiomyocytes. Cell Rep 32:107925. https://doi.org/10.1016/j.celrep.2020.107925
13. Foteinou PT, Greenstein JL, Winslow RL (2015) Mechanistic investigation of the arrhythmogenic role of oxidized CaMKII in the heart. Biophys J 109:838–849. https://doi.org/10.1016/j.bpj.2015.06.064
14. Fowler ED, Wang N, Hezzell M, Chanoit G, Hancox JC, Cannell MB (2020) Arrhythmogenic late Ca^{2+} sparks in failing heart cells and their control by action potential configuration. Proc Natl Acad Sci USA 117:2687–2692. https://doi.org/10.1073/pnas.1918649117
15. Hafstad AD, Nabeebaccus AA, Shah AM (2013) Novel aspects of ROS signalling in heart failure. Basic Res Cardiol 108:359. https://doi.org/10.1007/s00395-013-0359-8
16. Hamilton S, Terentyev D (2018) Proarrhythmic remodeling of calcium homeostasis in cardiac disease; implications for diabetes and obesity. Front Physiol 9:1517. https://doi.org/10.3389/fphys.2018.01517
17. Hamilton S, Terentyeva R, Clements RT, Belevych AE, Terentyev D (2021) Sarcoplasmic reticulum-mitochondria communication; implications for cardiac arrhythmia. J Mol Cell Cardiol 156:105–113. https://doi.org/10.1016/j.yjmcc.2021.04.002
18. Hamilton S, Terentyeva R, Martin B, Perger F, Li J, Stepanov A, Bonilla IM, Knollmann BC, Radwanski PB, Gyorke S, Belevych AE, Terentyev D (2020) Increased RyR2 activity is exacerbated by calcium leak-induced mitochondrial ROS. Basic Res Cardiol 115:38. https://doi.org/10.1007/s00395-020-0797-z
19. Hegyi B, Banyasz T, Izu LT, Belardinelli L, Bers DM, Chen-Izu Y (2018) β-adrenergic regulation of late Na^+ current during cardiac action potential is mediated by both PKA and CaMKII. J Mol Cell Cardiol 123:168–179. https://doi.org/10.1016/j.yjmcc.2018.09.006
20. Hegyi B, Bers DM, Bossuyt J (2019) CaMKII signaling in heart diseases: emerging role in diabetic cardiomyopathy. J Mol Cell Cardiol 127:246–259. https://doi.org/10.1016/j.yjmcc.2019.01.001
21. Hegyi B, Borst JM, Bailey LRJ, Shen EY, Lucena AJ, Navedo MF, Bossuyt J, Bers DM (2020) Hyperglycemia regulates cardiac K^+ channels via O-GlcNAc-CaMKII and NOX2-ROS-PKC pathways. Basic Res Cardiol 115:71. https://doi.org/10.1007/s00395-020-00834-8
22. Hegyi B, Bossuyt J, Ginsburg KS, Mendoza LM, Talken L, Ferrier WT, Pogwizd SM, Izu LT, Chen-Izu Y, Bers DM (2018) Altered repolarization reserve in failing rabbit ventricular myocytes: calcium and β-adrenergic effects on delayed- and inward-rectifier potassium currents. Circ Arrhythm Electrophysiol 11:e005852. https://doi.org/10.1161/CIRCEP.117.005852
23. Hegyi B, Bossuyt J, Griffiths LG, Shimkunas R, Coulibaly Z, Jian Z, Grimsrud KN, Sondergaard CS, Ginsburg KS, Chiamvimonvat N, Belardinelli L, Varro A, Papp JG, Pollesello P, Levijoki J, Izu LT, Boyd WD, Banyasz T, Bers DM, Chen-Izu Y (2018) Complex electrophysiological remodeling in postinfarction ischemic heart failure. Proc Natl Acad Sci USA 115:E3036–E3044. https://doi.org/10.1073/pnas.1718211115
24. Hegyi B, Chen-Izu Y, Izu LT, Rajamani S, Belardinelli L, Bers DM, Banyasz T (2020) Balance between rapid delayed rectifier K^+ Current and late Na^+ current on ventricular repolarization: an effective antiarrhythmic target? Circ Arrhythm Electrophysiol 13:e008130. https://doi.org/10.1161/CIRCEP.119.008130
25. Hegyi B, Fasoli A, Ko CY, Van BW, Alim CC, Shen EY, Ciccozzi MM, Tapa S, Ripplinger CM, Erickson JR, Bossuyt J, Bers DM (2021) CaMKII serine 280 O-GlcNAcylation links diabetic hyperglycemia to proarrhythmia. Circ Res 129:98–113. https://doi.org/10.1161/CIRCRESAHA.120.318402
26. Hegyi B, Ko CY, Bossuyt J, Bers DM (2021) Two-hit mechanism of cardiac arrhythmias in diabetic hyperglycemia: reduced repolarization reserve, neurohormonal stimulation and heart failure exacerbate susceptibility. Cardiovasc Res. https://doi.org/10.1093/cvr/cvab006
27. Hegyi B, Morotti S, Liu C, Ginsburg KS, Bossuyt J, Belardinelli L, Izu LT, Chen-Izu Y, Banyasz T, Grandi E, Bers DM (2019) Enhanced depolarization drive in failing rabbit ventricular myocytes: calcium-dependent and β-adrenergic effects on late sodium, L-type calcium, and sodium-calcium exchange currents. Circ Arrhythm Electrophysiol 12:e007061. https://doi.org/10.1161/CIRCEP.118.007061
28. Hoeker GS, Hanafy MA, Oster RA, Bers DM, Pogwizd SM (2016) Reduced arrhythmia inducibility with calcium/calmodulin-dependent protein kinase II inhibition in heart failure rabbits. J Cardiovasc Pharmacol 67:260–265. https://doi.org/10.1097/FJC.0000000000000343
29. Horvath B, Banyasz T, Jian Z, Hegyi B, Kistamas K, Nanasi PP, Izu LT, Chen-Izu Y (2013) Dynamics of the late Na^+ current during cardiac action potential and its contribution to afterdepolarizations. J Mol Cell Cardiol 64:59–68. https://doi.org/10.1016/j.yjmcc.2013.08.010
30. Horvath B, Hegyi B, Kistamas K, Vaczi K, Banyasz T, Magyar J, Szentandrassy N, Nanasi PP (2015) Cytosolic calcium changes affect the incidence of early afterdepolarizations in canine ventricular myocytes. Can J Physiol Pharmacol 93:527–534. https://doi.org/10.1139/cjpp-2014-0511
31. Hu RM, Tester DJ, Li R, Sun T, Peterson BZ, Ackerman MJ, Makielski JC, Tan BH (2018) Mexiletine rescues a mixed biophysical phenotype of the cardiac sodium channel arising from the SCN5A mutation, N406K, found in LQT3 patients. Channels (Austin) 12:176–186. https://doi.org/10.1080/19336950.2018.1475794
32. Hwang HS, Nitu FR, Yang Y, Walweel K, Pereira L, Johnson CN, Faggioni M, Chazin WJ, Laver D, George AL Jr, Cornea RL, Bers DM, Knollmann BC (2014) Divergent regulation of ryanodine receptor 2 calcium release channels by arrhythmogenic human calmodulin missense mutants. Circ Res 114:1114–1124. https://doi.org/10.1161/CIRCRESAHA.114.303391
33. Jost N, Virag L, Bitay M, Takacs J, Lengyel C, Biliczki P, Nagy Z, Bogats G, Lathrop DA, Papp JG, Varro A (2005) Restricting excessive cardiac action potential and QT prolongation: a vital role for I_{Ks} in human ventricular muscle. Circulation 112:1392–1399. https://doi.org/10.1161/CIRCULATIONAHA.105.550111
34. Kornyeyev D, El-Bizri N, Hirakawa R, Nguyen S, Viatchenko-Karpinski S, Yao L, Rajamani S, Belardinelli L (2016) Contribution of the late sodium current to intracellular sodium and calcium overload in rabbit ventricular myocytes treated by anemone toxin. Am J Physiol Heart Circ Physiol 310:H426-435. https://doi.org/10.1152/ajpheart.00520.2015
35. Kryshtal DO, Blackwell DJ, Egly CL, Smith AN, Batiste SM, Johnston JN, Laver DR, Knollmann BC (2021) RYR2 channel inhibition is the principal mechanism of flecainide action in

CPVT. Circ Res 128:321–331. https://doi.org/10.1161/CIRCRESAHA.120.316819
36. Kwong JQ, Lu X, Correll RN, Schwanekamp JA, Vagnozzi RJ, Sargent MA, York AJ, Zhang J, Bers DM, Molkentin JD (2015) The mitochondrial calcium uniporter selectively matches metabolic output to acute contractile stress in the heart. Cell Rep 12:15–22. https://doi.org/10.1016/j.celrep.2015.06.002
37. Li Q, Su D, O'Rourke B, Pogwizd SM, Zhou L (2015) Mitochondria-derived ROS bursts disturb Ca^{2+} cycling and induce abnormal automaticity in guinea pig cardiomyocytes: a theoretical study. Am J Physiol Heart Circ Physiol 308:H623-636. https://doi.org/10.1152/ajpheart.00493.2014
38. Liu N, Ruan Y, Denegri M, Bachetti T, Li Y, Colombi B, Napolitano C, Coetzee WA, Priori SG (2011) Calmodulin kinase II inhibition prevents arrhythmias in $RyR2^{R4496C+/-}$ mice with catecholaminergic polymorphic ventricular tachycardia. J Mol Cell Cardiol 50:214–222. https://doi.org/10.1016/j.yjmcc.2010.10.001
39. Liu T, Brown DA, O'Rourke B (2010) Role of mitochondrial dysfunction in cardiac glycoside toxicity. J Mol Cell Cardiol 49:728–736. https://doi.org/10.1016/j.yjmcc.2010.06.012
40. Liu T, Yang N, Sidor A, O'Rourke B (2021) MCU overexpression rescues inotropy and reverses heart failure by reducing SR Ca^{2+} leak. Circ Res 128:1191–1204. https://doi.org/10.1161/CIRCRESAHA.120.318562
41. Lu S, Liao Z, Lu X, Katschinski DM, Mercola M, Chen J, Heller Brown J, Molkentin JD, Bossuyt J, Bers DM (2020) Hyperglycemia acutely increases cytosolic reactive oxygen species via O-linked GlcNAcylation and CaMKII activation in mouse ventricular myocytes. Circ Res 126:e80–e96. https://doi.org/10.1161/CIRCRESAHA.119.316288
42. Maack C, Cortassa S, Aon MA, Ganesan AN, Liu T, O'Rourke B (2006) Elevated cytosolic Na^+ decreases mitochondrial Ca^{2+} uptake during excitation-contraction coupling and impairs energetic adaptation in cardiac myocytes. Circ Res 99:172–182. https://doi.org/10.1161/01.RES.0000232546.92777.05
43. Maltsev VA, Sabbah HN, Higgins RS, Silverman N, Lesch M, Undrovinas AI (1998) Novel, ultraslow inactivating sodium current in human ventricular cardiomyocytes. Circulation 98:2545–2552. https://doi.org/10.1161/01.cir.98.23.2545
44. McKeithan WL, Feyen DAM, Bruyneel AAN, Okolotowicz KJ, Ryan DA, Sampson KJ, Potet F, Savchenko A, Gomez-Galeno J, Vu M, Serrano R, George AL Jr, Kass RS, Cashman JR, Mercola M (2020) Reengineering an antiarrhythmic drug using patient hiPSC cardiomyocytes to improve therapeutic potential and reduce toxicity. Cell Stem Cell 27:813–821. https://doi.org/10.1016/j.stem.2020.08.003
45. Morotti S, Grandi E (2019) Quantitative systems models illuminate arrhythmia mechanisms in heart failure: role of the Na^+-Ca^{2+}-Ca^{2+}/calmodulin-dependent protein kinase II-reactive oxygen species feedback. Wiley Interdiscip Rev Syst Biol Med 11:e1434. https://doi.org/10.1002/wsbm.1434
46. Nabauer M, Kaab S (1998) Potassium channel down-regulation in heart failure. Cardiovasc Res 37:324–334. https://doi.org/10.1016/s0008-6363(97)00274-5
47. Nattel S, Heijman J, Zhou L, Dobrev D (2020) Molecular basis of atrial fibrillation pathophysiology and therapy: a translational perspective. Circ Res 127:51–72. https://doi.org/10.1161/CIRCRESAHA.120.316363
48. Nemec J, Kim JJ, Salama G (2016) The link between abnormal calcium handling and electrical instability in acquired long QT syndrome–does calcium precipitate arrhythmic storms? Prog Biophys Mol Biol 120:210–221. https://doi.org/10.1016/j.pbiomolbio.2015.11.003
49. Nishio S, Teshima Y, Takahashi N, Thuc LC, Saito S, Fukui A, Kume O, Fukunaga N, Hara M, Nakagawa M, Saikawa T (2012) Activation of CaMKII as a key regulator of reactive oxygen species production in diabetic rat heart. J Mol Cell Cardiol 52:1103–1111. https://doi.org/10.1016/j.yjmcc.2012.02.006
50. Oda T, Yang Y, Uchinoumi H, Thomas DD, Chen-Izu Y, Kato T, Yamamoto T, Yano M, Cornea RL, Bers DM (2015) Oxidation of ryanodine receptor (RyR) and calmodulin enhance Ca release and pathologically alter, RyR structure and calmodulin affinity. J Mol Cell Cardiol 85:240–248. https://doi.org/10.1016/j.yjmcc.2015.06.009
51. Parikh A, Mantravadi R, Kozhevnikov D, Roche MA, Ye Y, Owen LJ, Puglisi JL, Abramson JJ, Salama G (2012) Ranolazine stabilizes cardiac ryanodine receptors: a novel mechanism for the suppression of early afterdepolarization and torsades de pointes in long QT type 2. Heart Rhythm 9:953–960. https://doi.org/10.1016/j.hrthm.2012.01.010
52. Perez-Hernandez M, Leo-Macias A, Keegan S, Jouni M, Kim JC, Agullo-Pascual E, Vermij S, Zhang M, Liang FX, Burridge P, Fenyo D, Rothenberg E, Delmar M (2021) Structural and functional characterization of a Nav1.5-mitochondrial couplon. Circ Res 128:419–432. https://doi.org/10.1161/CIRCRESAHA.120.318239
53. Pogwizd SM, Qi M, Yuan W, Samarel AM, Bers DM (1999) Upregulation of Na^+/Ca^{2+} exchanger expression and function in an arrhythmogenic rabbit model of heart failure. Circ Res 85:1009–1019. https://doi.org/10.1161/01.res.85.11.1009
54. Pogwizd SM, Schlotthauer K, Li L, Yuan W, Bers DM (2001) Arrhythmogenesis and contractile dysfunction in heart failure: roles of sodium-calcium exchange, inward rectifier potassium current, and residual beta-adrenergic responsiveness. Circ Res 88:1159–1167. https://doi.org/10.1161/hh1101.091193
55. Qu Z, Xie LH, Olcese R, Karagueuzian HS, Chen PS, Garfinkel A, Weiss JN (2013) Early afterdepolarizations in cardiac myocytes: beyond reduced repolarization reserve. Cardiovasc Res 99:6–15. https://doi.org/10.1093/cvr/cvt104
56. Ronchi C, Torre E, Rizzetto R, Bernardi J, Rocchetti M, Zaza A (2017) Late sodium current and intracellular ionic homeostasis in acute ischemia. Basic Res Cardiol 112:12. https://doi.org/10.1007/s00395-017-0602-9
57. Santulli G, Xie W, Reiken SR, Marks AR (2015) Mitochondrial calcium overload is a key determinant in heart failure. Proc Natl Acad Sci USA 112:11389–11394. https://doi.org/10.1073/pnas.1513047112
58. Shannon TR, Pogwizd SM, Bers DM (2003) Elevated sarcoplasmic reticulum Ca^{2+} leak in intact ventricular myocytes from rabbits in heart failure. Circ Res 93:592–594. https://doi.org/10.1161/01.RES.0000093399.11734.B3
59. Sossalla S, Fluschnik N, Schotola H, Ort KR, Neef S, Schulte T, Wittkopper K, Renner A, Schmitto JD, Gummert J, El-Armouche A, Hasenfuss G, Maier LS (2010) Inhibition of elevated Ca^{2+}/calmodulin-dependent protein kinase II improves contractility in human failing myocardium. Circ Res 107:1150–1161. https://doi.org/10.1161/CIRCRESAHA.110.220418
60. Spencer CI, Baba S, Nakamura K, Hua EA, Sears MA, Fu CC, Zhang J, Balijepalli S, Tomoda K, Hayashi Y, Lizarraga P, Wojciak J, Scheinman MM, Aalto-Setala K, Makielski JC, January CT, Healy KE, Kamp TJ, Yamanaka S, Conklin BR (2014) Calcium transients closely reflect prolonged action potentials in iPSC models of inherited cardiac arrhythmia. Stem Cell Rep 3:269–281. https://doi.org/10.1016/j.stemcr.2014.06.003
61. Swaminathan PD, Purohit A, Hund TJ, Anderson ME (2012) Calmodulin-dependent protein kinase II: linking heart failure and arrhythmias. Circ Res 110:1661–1677. https://doi.org/10.1161/CIRCRESAHA.111.243956
62. Terentyev D, Gyorke I, Belevych AE, Terentyeva R, Sridhar A, Nishijima Y, de Blanco EC, Khanna S, Sen CK, Cardounel AJ, Carnes CA, Gyorke S (2008) Redox modification of ryanodine

receptors contributes to sarcoplasmic reticulum Ca^{2+} leak in chronic heart failure. Circ Res 103:1466–1472. https://doi.org/10.1161/CIRCRESAHA.108.184457

63. Terentyev D, Rees CM, Li W, Cooper LL, Jindal HK, Peng X, Lu Y, Terentyeva R, Odening KE, Daley J, Bist K, Choi BR, Karma A, Koren G (2014) Hyperphosphorylation of RyRs underlies triggered activity in transgenic rabbit model of LQT2 syndrome. Circ Res 115:919–928. https://doi.org/10.1161/CIRCRESAHA.115.305146
64. Uchinoumi H, Yang Y, Oda T, Li N, Alsina KM, Puglisi JL, Chen-Izu Y, Cornea RL, Wehrens XHT, Bers DM (2016) CaMKII-dependent phosphorylation of RyR2 promotes targetable pathological RyR2 conformational shift. J Mol Cell Cardiol 98:62–72. https://doi.org/10.1016/j.yjmcc.2016.06.007
65. Valdivia CR, Chu WW, Pu J, Foell JD, Haworth RA, Wolff MR, Kamp TJ, Makielski JC (2005) Increased late sodium current in myocytes from a canine heart failure model and from failing human heart. J Mol Cell Cardiol 38:475–483. https://doi.org/10.1016/j.yjmcc.2004.12.012
66. Viatchenko-Karpinski S, Kornyeyev D, El-Bizri N, Budas G, Fan P, Jiang Z, Yang J, Anderson ME, Shryock JC, Chang CP, Belardinelli L, Yao L (2014) Intracellular Na^+ overload causes oxidation of CaMKII and leads to Ca^{2+} mishandling in isolated ventricular myocytes. J Mol Cell Cardiol 76:247–256. https://doi.org/10.1016/j.yjmcc.2014.09.009
67. Wagner S, Dybkova N, Rasenack EC, Jacobshagen C, Fabritz L, Kirchhof P, Maier SK, Zhang T, Hasenfuss G, Brown JH, Bers DM, Maier LS (2006) Ca2+/calmodulin-dependent protein kinase II regulates cardiac Na^+ channels. J Clin Invest 116:3127–3138. https://doi.org/10.1172/JCI26620
68. Wagner S, Maier LS, Bers DM (2015) Role of sodium and calcium dysregulation in tachyarrhythmias in sudden cardiac death. Circ Res 116:1956–1970. https://doi.org/10.1161/CIRCRESAHA.116.304678
69. Wagner S, Ruff HM, Weber SL, Bellmann S, Sowa T, Schulte T, Anderson ME, Grandi E, Bers DM, Backs J, Belardinelli L, Maier LS (2011) Reactive oxygen species-activated Ca/calmodulin kinase IIδ is required for late I_{Na} augmentation leading to cellular Na and Ca overload. Circ Res 108:555–565. https://doi.org/10.1161/CIRCRESAHA.110.221911
70. Willis BC, Pandit SV, Ponce-Balbuena D, Zarzoso M, Guerrero-Serna G, Limbu B, Deo M, Camors E, Ramirez RJ, Mironov S, Herron TJ, Valdivia HH, Jalife J (2016) Constitutive intracellular Na^+ excess in Purkinje cells promotes arrhythmogenesis at lower levels of stress than ventricular myocytes from mice with catecholaminergic polymorphic ventricular tachycardia. Circulation 133:2348–2359. https://doi.org/10.1161/CIRCULATIONAHA.116.021936
71. Xie LH, Chen F, Karagueuzian HS, Weiss JN (2009) Oxidative-stress-induced afterdepolarizations and calmodulin kinase II signaling. Circ Res 104:79–86. https://doi.org/10.1161/CIRCRESAHA.108.183475
72. Yao L, Fan P, Jiang Z, Viatchenko-Karpinski S, Wu Y, Kornyeyev D, Hirakawa R, Budas GR, Rajamani S, Shryock JC, Belardinelli L (2011) Nav1.5-dependent persistent Na^+ influx activates CaMKII in rat ventricular myocytes and N1325S mice. Am J Physiol Cell Physiol 301:C577-586. https://doi.org/10.1152/ajpcell.00125.2011